

Dissecting inherent intratumor heterogeneity in patient-derived glioblastoma culture models

Jian Teng,[#] Cintia Carla da Hora,[#] Rami S. Kantar, Ichiro Nakano, Hiroaki Wakimoto, Tracy T. Batchelor, E. Antonio Chiocca, Christian E. Badr,[†] and Bakhos A. Tannous[†]

Experimental Therapeutics and Molecular Imaging Laboratory (J.T., C.C.H., R.S.K., C.E.B., B.A.T.); Department of Neurology, Neuro-Oncology Division, Massachusetts General Hospital, Boston, Massachusetts (J.T., C.C.H., R.S.K., T.T.B., C.E.B., B.A.T.); Neuroscience Program, Harvard Medical School, Boston, Massachusetts (J.T., C.C.H., R.S.K., C.E.B., B.A.T.); Department of Neurological Surgery, The Ohio State University, Columbus, Ohio (I.N.); Department of Neurosurgery, Massachusetts General Hospital, Boston, Massachusetts (H.W.); Massachusetts General Hospital Cancer Center, Boston, Massachusetts (T.T.B.); Department of Neurosurgery, Brigham and Women's Hospital, Boston, Massachusetts (E.A.C.)

Corresponding Authors: Bakhos A. Tannous, Ph.D., Experimental Therapeutics and Molecular Imaging Laboratory, Massachusetts General Hospital, Building 149, 13th Street, Charlestown, MA, 02129 USA (btannous@hms.harvard.edu). Christian E. Badr, Ph.D., Department of Neurology, Massachusetts General Hospital, Building 149, 13th Street, Charlestown, MA, 02129 USA (badr.christian@mgh.harvard.edu).

[#]These authors contributed equally to the manuscript.

[†]Co-senior authors.

Abstract

Background. Molecular profile of glioblastoma multiforme (GBM) revealed 4 subtypes, 2 of which, proneural and mesenchymal, have been predominantly observed, with the latter displaying a more aggressive phenotype and increased therapeutic resistance. Single-cell RNA sequencing revealed that multiple subtypes actually reside within the same tumor, suggesting cellular heterogeneity in GBM. Further, plasticity between these 2 subtypes is observed during tumor recurrence and in response to radiation therapy.

Methods. Patient-derived GBM stemlike cells were cultured as neurospheres. These cells were differentiated in serum by attaching to the culture dishes. The “floating” cells that were not attached/differentiated were harvested from the conditioned medium. The characteristics of these cells were studied with limiting dilution assays and immunofluorescence staining. Cell growth and nuclear factor-kappaB (NFkB) activation were monitored using bioluminescent assays as well as quantitative polymerase chain reaction and western blotting. In vivo tumorigenesis was evaluated in orthotopic xenograft models using bioluminescence imaging.

Results. Patient-derived GBM stemlike cells undergo differentiation by attaching to the culture dish in serum-containing medium. We observed that a small subset of these cells escape this adhesion/differentiation and grow as floating cells. These cells displayed enhanced cancer stem cell properties with a molecular and phenotypic mesenchymal signature, including resistance to radiation and targeted therapies, a more aggressive tumor formation, and NFkB activation.

Conclusion. Our results endorse inherent intratumor molecular subtype heterogeneity in glioblastoma and provide a valuable approach to study phenotypic plasticity, which could be applied to find novel therapeutic strategies to eradicate this aggressive tumor and can be extended to other cancer types.

Key words

cancer stem cells | differentiation | glioblastoma | intratumor heterogeneity | mesenchymal transition

Importance of the study

We characterized a subpopulation of glioblastoma stem cells that escape adhesion/differentiation conditions and have enhanced cancer stem cell properties. These cells display stemlike properties with a molecular and phenotypic mesenchymal signature, including

resistance to radiation and targeted therapies, a more aggressive tumor formation, and NF κ B activation. Our results endorse cellular plasticity and intratumor molecular subtype heterogeneity in glioblastoma, which could have significant clinical implications.

Glioblastoma (GBM), the most common primary malignant brain tumor,^{1,2} presents a heterogeneous cell population with typical cellular hierarchies, complicating the effort to target and eradicate the entire tumor.³ Substantial evidence suggests that GBM contains a small subpopulation with distinct stemlike properties, referred to as glioma stem cells (GSCs) or tumor initiating cells, which play an important role in GBM initiation, progression, invasion, and therapeutic resistance.⁴ These cells can divide asymmetrically with one cell producing an identical daughter cell and a more differentiated cell, thus causing the heterogeneous lineage in tumor. The GSC hypothesis offers a valuable model to study the etiology of GBM and identify potential therapeutics owing to GSCs' abilities of self-renewal, differentiation, and recapitulation of the original tumor upon xenotransplantation.^{2,5,6} Molecular classification of GBM identified 4 subtypes, 2 of which, proneural (PN) and mesenchymal (MES), have been predominantly observed.^{7,8} GBM tumors with MES properties typically display a more aggressive phenotype both in vitro and in vivo, along with a pronounced radioresistance.^{7,9} Recently, single-cell RNA sequencing revealed that multiple subtypes actually reside within the same tumor,¹⁰ suggesting cellular heterogeneity in GBM. Further, proneural tumors tend to shift toward a MES phenotype upon recurrence, or in response to radiation therapy.^{7,9,11,12} GSCs with a predominant proneural signature can undergo MES transition through intrinsic activation of various transcription factors such as signal transducer and activator of transcription 3 (STAT3), CCAAT-enhancer binding homologous protein beta (C/EBP β), transcriptional coactivator with PDZ-binding motif (TAZ), Twist-related protein 1, and nuclear factor- κ B (NF κ B).^{13,14} Such transition may reflect different stages at which the ancestral cell has undergone its neoplastic transformation.^{7,9}

GSCs are typically enriched in serum-free media as suspended neurospheres. When these cells are maintained in serum-containing medium, they undergo dramatic alterations in genotype, morphology, and adhesion properties and lose the ability to generate secondary spheres, thus are poor models for cancer.¹⁵⁻¹⁷ Here, we show that a subpopulation of GBM cells escape the serum-induced adhesion/differentiation and undergo mesenchymal switch with enhanced cancer stem cell properties, attesting to inherent intratumoral heterogeneity in GBM. These findings provide a valuable approach to understand tumor heterogeneity and cellular plasticity in GBM and to develop novel therapeutic strategies against this aggressive tumor type.

Materials and Methods

Cell Culture, Constructions and Reagents

Primary GSCs used in this study were derived from surgical specimens obtained from glioblastoma patients undergoing treatment at the Massachusetts General Hospital or The Ohio State University James Comprehensive Cancer Center, in accordance with the appropriate institutional review board approval, and have been previously characterized.^{9,18,19} GSCs are cultured as neurospheres in serum-free neurobasal medium supplemented with human recombinant epidermal growth factor and basic fibroblast growth factor (NBM). For bioluminescence imaging, cells were transduced with the CSCW-Fluc-IRES-mCherry lentivirus vector carrying an expression cassette for firefly luciferase (Fluc) and mCherry fluorescent protein.²⁰ Temozolomide was purchased from Sigma Aldrich. Detailed methods for different experiments can be found in the Supplementary material.

Immunocytochemistry

Cells were plated on Nunc Lab-tek II chamber slides (Sigma-Aldrich), in the presence of Synthemax II-SC substrate (1 μ g/mL to attach the GSC spheres). Cells were fixed with 4% paraformaldehyde for 30 min, permeabilized with 0.3% Triton X100 for 5 min, and blocked with 10% goat serum (Vector Laboratories). Cells were then incubated for 2 h at 37°C with monoclonal mouse anti-oligodendrocyte marker O4 (Olig4, 1:50; R&D Systems), neuron-specific beta III tubulin (TUBB3, 1:100; Abcam), polyclonal mouse anti-gliial fibrillary acidic protein (GFAP, 1:50; Stemcell Technologies), rabbit SRY (sex determining region Y)-box 2 (Sox2, 1:50; Stemgent), and mouse cluster of differentiation (CD)44 (1:100, Cell Signaling). Complementary secondary antibody conjugated to a fluorophore (1:100, Life Technologies) was then added and incubated for 1 h. Cells were washed and nuclei were counterstained with 4',6'-diamidino-2-phenylindole, mounted on a microscope slide, and analyzed by fluorescence microscopy.

Scratch Wound Healing Assay for Cell Migration

A monolayer of neurospheres (NS) and floating cell spheres (FC) cultured in the presence of 1 μ g/mL Synthemax II-SC substrate (Corning) were scratched using a pipette tip to create a wound. Cells migrating from the leading edge were photographed at different time points

using phase-contrast microscopy. Distance was measured in 10 \times field using ImageJ (National Institutes of Health).

Flow Cytometry

For cell cycle analysis, cells were washed and fixed in 70% ethanol and incubated in phosphate buffered saline (PBS) containing 40 μ g/mL propidium iodide and 200 μ g/mL RNase A (New England Biolabs). DNA content was analyzed by flow cytometry. CD44 expression was measured in 500 000 cells dissociated with 2 mM EDTA and incubated in 80 μ L PBS/0.1% bovine serum albumin at 4°C for 30 min in the dark with mouse monoclonal anti-human CD44 antibody conjugated to fluorescein isothiocyanate (FITC, 1:10; Miltenyi Biotec) or respective mouse immunoglobulin G1 control in the presence of FcR blocking reagent (1:5). FITC was then analyzed with a LSR II Flow Cytometer System (BD Biosciences).

Mesenchymal Differentiation Assay

Differentiation of cells was performed using the StemPro Chondrogenesis Differentiation Kit (Life Technologies). Briefly, 2.5 \times 10⁵ NS or FC were cultured in osteocyte/chondrocyte basal medium supplemented with chondrogenesis supplement. After 21 days in culture, osteocytes/chondrocytes were stained with fast green and safranin O following the standard protocol.

Evaluation of NF κ B Activity

NS were transduced with 2 lentiviral vectors expressing (i) secreted *Gaussia* luciferase (Gluc) under tandem repeats of the NF κ B transcription responsive elements and (ii) secreted *Vargula hilgendorffii* luciferase (Vluc) under the control of the constitutively active SV40 promoter. These cells were differentiated in serum, and FC were collected from them and cultured as NS. Twenty-microliter aliquots of conditioned medium from each of NS and FC were assayed for Gluc activity (to measure NF κ B activity) and Vluc activity (to normalize for cell number) using coelenterazine and vargulin substrate, respectively, as we previously described.^{21,22} The normalized Gluc/Vluc ratio was then calculated as a marker for NF κ B activation.

In vivo Tumor Model

All animal studies were approved by the Massachusetts General Hospital Subcommittee on Research Animal Care following guidelines set forth by the National Institutes of Health Guide for the Care and Use of Laboratory Animals. Female nude mice were anesthetized (100 mg/kg ketamine and 5 mg/kg xylazine) and stereotactically implanted with 5 \times 10⁴ GBM cells (as small spheres) expressing Fluc in 2 μ L PBS via a 30-gauge Hamilton syringe into the left forebrain. Bioluminescence imaging was performed using the Xenogen IVIS 200 Imaging System (PerkinElmer) as we previously described.²³

Statistical Analysis

GraphPad Prism v6.01 software was used for statistical analysis of all data. $P < .05$ was considered to be statistically significant. For analysis between multiple groups, a 1-way ANOVA was performed followed by Sidak's multiple comparison test to compare differences between 2 groups. An unpaired 2-tailed t -test was used for the comparison of 2 samples. Survival was analyzed using Kaplan–Meier curves and log-rank (Mantel–Cox) tests.

Results

A Subset of Patient-Derived GBM Stem Cells Escapes Differentiation Conditions and Forms Neurospheres in Culture

Patient-derived GBM stem cells (NS) undergo differentiation in culture by attaching to the culture dish in serum-containing medium or in the presence of other differentiating agents. Nonetheless, we observed that a small subset of these cells appears to escape adhesion/differentiation conditions and grow as FC (Fig. 1A; Supplementary Fig. S1A). We therefore raised the hypothesis that serum conditions yield in fact 2 different subpopulations. When these FC were separated from attached cells and cultured in serum, they showed to be fully viable (Supplementary Fig. S1B). When cultured in serum-free NBM, small 3-dimensional spheroids emerged (Fig. 1A). These FC grew gradually over time and could be maintained and passaged as NS. On the other hand, when the adherent cell (AC) population were detached and resuspended in NBM, these cells formed small clusters which were more likely to be aggregates of cells, not morphologically spheres, and failed to generate secondary spheres (Fig. 1A).

To investigate the ability of FC to form viable spheres, we used 8 well-characterized patient-derived GSC cultures (MGG6, MGG8, MGG23, MGG29, 84, 157, BT01, and BT07), which we have subtyped based on established gene expression profile (Supplementary Table S1).^{9,18,19} One thousand single cells dissociated from NS as well as their corresponding AC and FC were cultured in NBM. After one week, we applied the extreme limiting dilution analysis (ELDA) algorithm²⁴ to calculate stem cell frequency and observed that FC had a significantly higher sphere formation frequency compared with NS ($P < .01$), while sphere formation by AC was ineffective (Fig. 1B). In addition, we found that FC collected from U87MG and U251MG cell lines could grow and form secondary spheres in a similar frequency.

We noted that FC were especially abundant after AC being cultured in Dulbecco's modified Eagle's medium with fetal bovine serum (DMEM-FBS) for 4 to 5 days, and we sought to determine whether this phenomenon was due to the reduced pH in the medium, since previous studies have demonstrated that acidic conditions can favor GSC growth.²⁵ When a fluorogenic intracellular pH indicator was added into the culture medium, FC but not AC showed fluorescence indicating that the intracellular pH in FC is significantly lower (Fig. 1C). Propidium iodide staining excluded

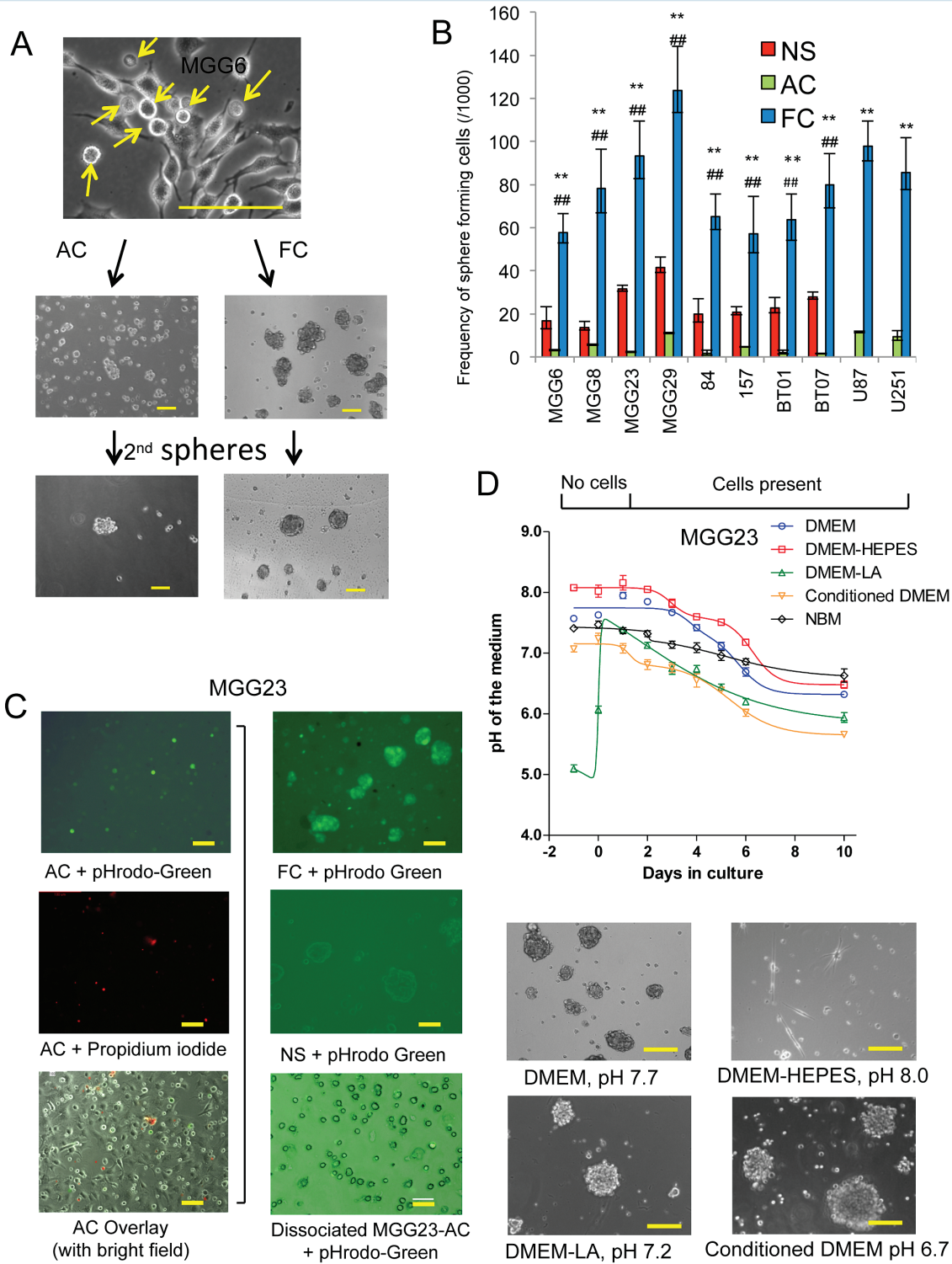


Fig. 1 Isolation of a floating cell population from differentiated GBM cells. (A) Bright field micrographs of GSCs cultured in DMEM-FBS. A large proportion of floating cells (FC) emerge from adherent cell (AC) cultures. FC and AC were then cultured in NBM and only FC can form spheres and secondary spheres. Arrow, FC population. (B) One thousand single cells of NS, AC, and FC from 8 different GSCs and 2 GBM cell lines were cultured. One week later, extreme limiting dilution analysis (ELDA) was applied with 12 replicates. Statistics for stem cell frequencies (with 95% CIs) in FC, AC, and the corresponding NS are shown. $**P < .01$ FC vs AC, $##P < 0.01$ NS vs FC. (C) Left panels: MGG23 cultured in DMEM-FBS and analyzed by fluorescence microscopy; upper, green showing low intracellular pH in FC; middle, propidium iodide staining; bottom, overlay with bright field image. Right: fluorescence analysis of MGG23 cells under different conditions; upper, MGG23 FC; middle, MGG23 NS; bottom, dissociated MGG23 AC. (D) Upper panel: pH in medium of MGG23 GSCs cultured in DMEM-FBS, DMEM-FBS with 25 mM of HEPES, DMEM-FBS with 15 mM lactic acid, conditioned medium, or NBM. Lower panels: bright field micrographs of FC collected under different conditions and cultured in NBM. Scale bar, 50 μ m.

that these cells could be dying or dead. In addition, secondary spheres formed from FC also showed substantially lower intracellular pH compared with their original NS (Fig. 1C). When AC were dissociated and suspended in medium containing pHrodo-Green, these cells did not show any fluorescent signal (Fig. 1C). We observed that DMEM-FBS (in the absence of cultured cells) had a slightly alkaline pH baseline (~7.9) after calibration in the standard CO₂ condition overnight (day 0) and gradually dropped to ~7.2 after 5 days and as low as ~6.5 after 8 days when conditioned by GBM cells (Fig. 1D, Supplementary Fig. S1A). When 25 mM HEPES (4-(2-hydroxyethyl)-1-piperazine ethanesulfonic acid) was added to the culture medium, pH was maintained at above 7.5 for at least 6 days. Interestingly, the FC population collected from HEPES-stabilized medium could not survive in NBM, with only a few differentiated cells attached to the plate (Fig. 1D). On the other hand, when 15 mM lactic acid, the biological metabolite in cellular respiration, was added to the medium, pH was reduced to ~6.5 and a large proportion of cells floated (Fig. 1D). We also evaluated the conditioned medium collected at day 5, which had a stable low pH at around 6.5–6.8, and showed that this medium can induce FC formation (Fig. 1D, Supplementary Fig. S1B). Since hypoxic conditions have also been implicated in GBM progression, we investigated the effect of low oxygen levels on FC formation. Interestingly, combination of acidic conditions with low oxygen enhanced both FC development as well as primary and secondary sphere formation compared with acidic conditions alone (Supplementary Fig. S2). These data suggest that acidic condition in combination with hypoxia facilitates the formation of FC and maintenance of sphere-forming cells from differentiated GBM cells in culture.

Floating Cell Spheres Retain Expression of Stem Cell Markers

To evaluate the stemlike properties of the FC population, we performed immunostaining for the stem cell representative marker Sox2 and a set of differentiation markers, including GFAP, Olig4, and TUBB3 in NS, FC, AC, and FC that were forced to differentiate in serum for >15 days (FC-AC). Similar to NS, FC exhibited positive immunoreactivity to Sox2, but no detectable immunoreactivity to GFAP, Olig4, or TUBB3. In contrast, both AC and FC-AC showed the opposite results (Fig. 2A and Supplementary Fig. S3). We also analyzed mRNA from these cells by quantitative real-time (qRT)-PCR for a panel of biomarkers and observed that the expression of 9 different stem cell markers—SOX2; OCT-4; Nestin; BMI-1; KLF-4; Nanog; CD133; Olig2; and Sox 11—were significantly higher in FC and in the parental NS, compared with their corresponding differentiated adherent cells (FC-AC and AC). In turn, an increased expression of differentiation markers (GFAP and TUBB3) was observed in FC-AC and AC (Fig. 2B, Supplementary Fig. S4A). These mRNA expression profiles were consistent with the protein expression patterns determined by western blotting. Elevated levels of GFAP, TUBB3 and NeuN (neuron nuclei protein) were observed in the differentiated cells, whereas NS and FC showed low-to-undetectable expression levels of these differentiation markers. Sox2, on the other hand, was enriched in FC and NS (Fig. 2C and Supplementary Fig. S4B).

Collectively these data suggest that FC retain the stemlike properties and can give rise to differentiated GBM cells.

Floating Cell Spheres Are Highly Tumorigenic In vivo

To evaluate the tumorigenic potential of FC compared with their parental NS, we stereotactically implanted 50000 cells of NS, AC, FC, or FC-AC from MGG6 stably expressing the Fluc reporter into the brain of athymic mice ($n = 7-10$ /group). Bioluminescence imaging showed that tumors formed by FC grew significantly faster compared with their corresponding NS tumors. At day 49, average Fluc activity in FC tumors was 204-fold higher compared with NS tumors ($P < .001$; Fig. 3A and B). Further, mice carrying FC-derived brain tumors had a significantly shorter survival compared with the NS group, with a median survival of 45 days for the FC group versus 55 days for the NS group ($P = .0008$; Fig. 3C). The differentiated AC and FC-AC, however, were incapable of forming any tumors with mice surviving >100 days. We repeated the same experiment using GSCs 157 NS and their FC counterpart and observed similar results (Fig. 3D–F). Hematoxylin and eosin staining showed that FC formed much more aggressive tumors, which was translated into a significantly shorter mice survival compared with the NS group (median survivals were 37.5 and 21.5 days for NS and FC groups, respectively; $P = .0015$; Fig. 3F and Supplementary Fig. S5A). In addition, FC isolated from U251MG glioma cell line (U251-FC) had a significantly higher tumor growth rate as compared with the parental U251MG cells ($P = .012$ at day 21; Supplementary Fig. S5B–C). Taken together, these data indicate that FCs induce an increased tumorigenic property in vivo.

Floating Cell Spheres Display Mesenchymal Properties

The ability of FC to survive and proliferate under extreme conditions (low pH and possibly low nutrients) along with their increased in vivo proliferation suggested a more aggressive tumor phenotype. A more detailed analysis of these 2 cell populations revealed a different molecular signature between NS and FC, with the latter exhibiting increased mesenchymal characteristics. The expression patterns of mesenchymal markers, including CD44, VIM, YKL-40, N-cad, MMP2,¹¹ and ALDH1A3 (recently characterized as a mesenchymal GSC marker)⁷ were elevated in all FC samples compared with their parental NS (Fig. 4A, Supplementary Fig. S6A). These results were confirmed in another set of FCs all showing higher CD44 expression compared with corresponding NS, irrespective of their original subtype (Supplementary Fig. S6B). FC enhanced MES phenotype was also confirmed through upregulation of CD44 protein as well as increased levels of phosphorylated-STAT3 (pSTAT3) in 3 different GSCs (MGG23, MGG6, and MGG8; Fig. 4B). C/EBP β was also increased in FC from MGG23 and MGG8 but was undetected in their parental NS (Fig. 4B). Fluorescence activated cell sorting (FACS) analysis confirmed that FC collected from 4 different GSC cultures (MGG6, MGG8, MGG23, and MGG29) have a significantly higher proportion of CD44 positive cells,

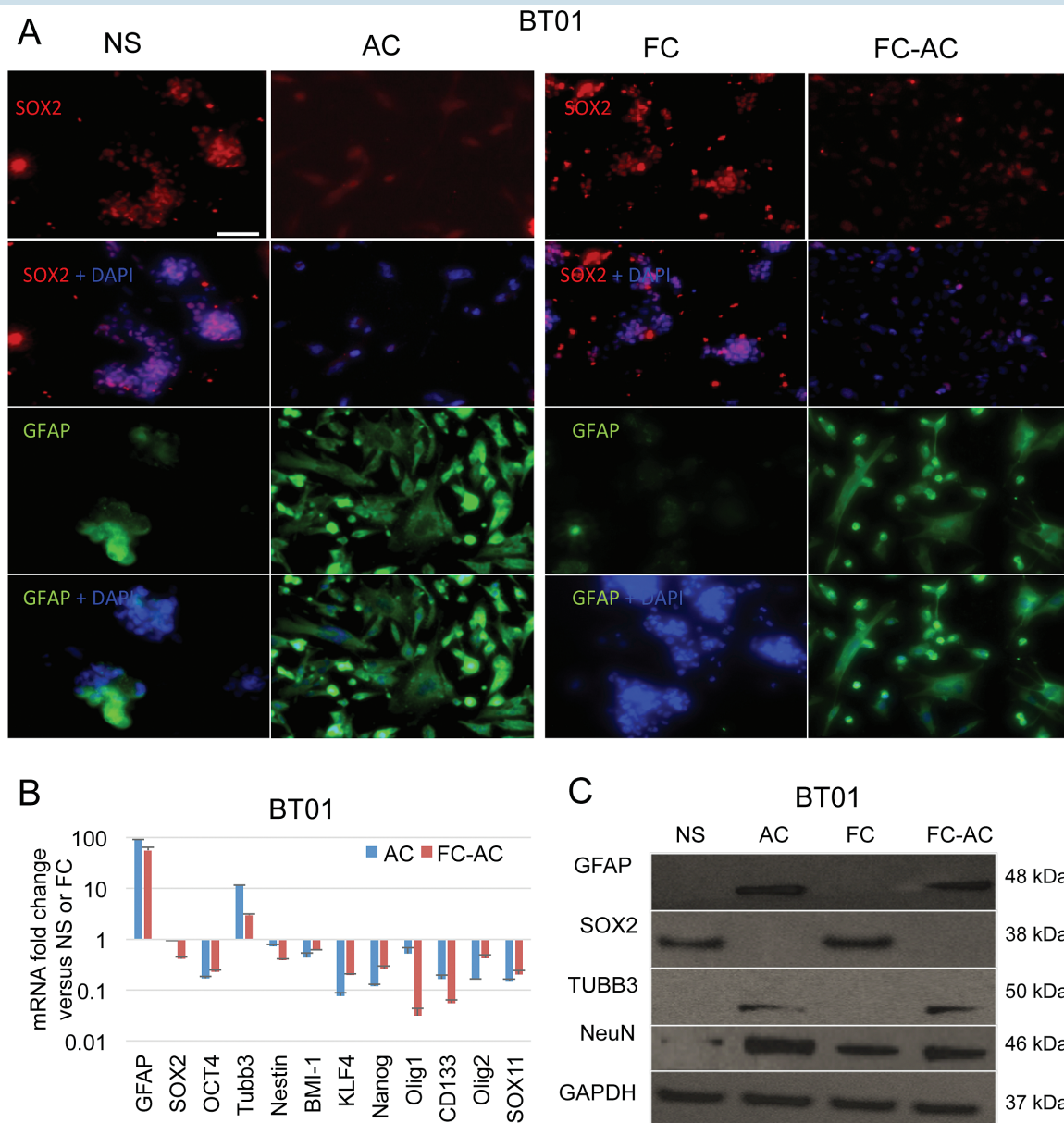


Fig. 2 Floating cells express stem cell markers. (A) BT01 GSCs NS and their corresponding AC, as well as FC spheres and their differentiated counterpart FC-AC were stained for Sox2, GFAP, and nuclei (using DAPI). Scale bar, 100 μ m. (B) mRNA expression profile of different genes in NS, FC, AC, and FC-AC from BT01 cells analyzed by qRT-PCR. Relative fold change of AC/NS and FC-AC/FC are shown. (C) Western blot analysis for GFAP, Sox2, TUBB3, NeuN, and GAPDH in cell lysates collected from NS, FC, AC, and FC-AC from BT01.

despite different CD44 expression levels in NS (Fig. 4C; Supplementary Table S1). Finally, increased expression of CD44 was maintained in FC upon xenotransplantation in mice brain (Supplementary Fig. S5A). These data collectively suggest that FC possess enhanced MES properties regardless of the originating GSC subtype.

We then asked whether higher mesenchymal markers in FC over NS are due to selection under culture condition or transformation of nonmesenchymal cells into a mesenchymal-like state. The cell surface marker CD44 is highly expressed in MES GBM and could be used as a surrogate marker for this subtype.⁷ We collected the viable CD44^{high} and CD44^{low} subpopulations of MGG29 NS by FACS and

labeled CD44^{high} cells with green fluorescent protein (GFP), and CD44^{low} cells with mCherry by transduction with corresponding lentivirus vectors (MGG29-CD44^{high}-GFP and MGG29-CD44^{low}-mCherry; Supplementary Fig. S7). These 2 subpopulations were then mixed together and cultured under serum conditions. When floating cells were collected from these cultures, we observed the presence of both GFP and mCherry expressing tumor cells. Flow cytometry analysis further showed that CD44^{high} cells can arise from both CD44^{low} cells and CD44^{high} cells altogether (Fig. 4D). To confirm the mesenchymal-like transdifferentiation, we applied an in vitro model using the mesenchymal stem cell chondrogenic differentiation kit on both MGG8 NS and

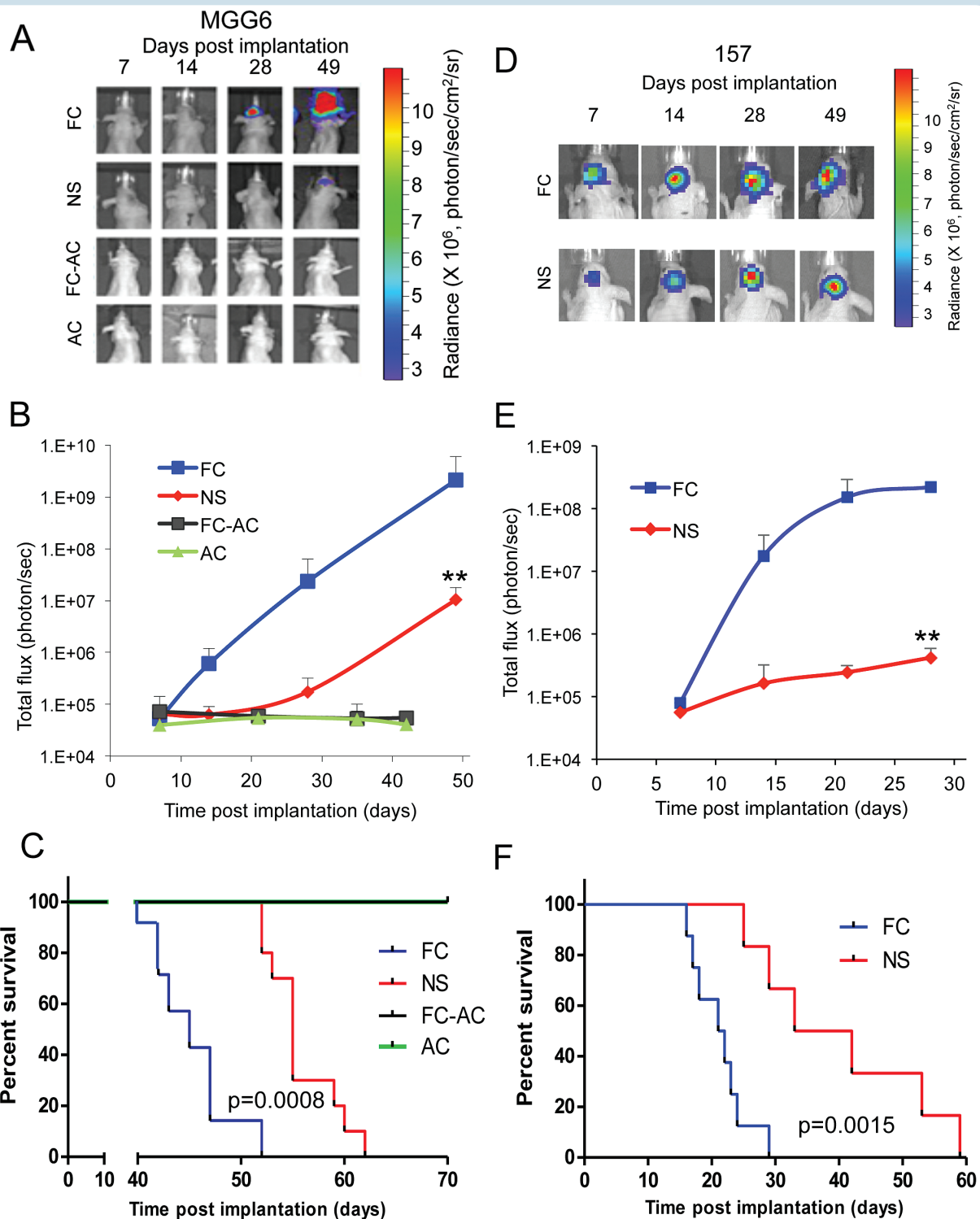


Fig. 3 Floating cells form aggressive tumors in vivo. (A–C) Athymic mice were implanted with ~50,000 of either FC, NS, FC-AC, or AC from MGG6 expressing Fluc into the left forebrain ($n=7-10$). Representative pseudo-color images of Fluc bioluminescence at different time point post-implantation (A). Quantification of Fluc radiance intensity presented as photons/sec/cm²/surface radiance; data presented as mean \pm SD, $n=10$, ** $P<.01$ FC vs NS by ANOVA and Tukey's post-hoc test (B). Kaplan–Meier survival curves; $n=7-10$; ** $P<.01$ FC vs NS by Mantel–Cox (log-rank) test (C). (D–F) Athymic mice were implanted with ~50,000 NS or FC cells from GSCs 157 and results were analyzed similar to A–C; $n=8$; ** $P<.01$ FC vs NS.

FC. Following 21 days of differentiation, cells were stained with fast green and safranin O. Interestingly, differentiated FC showed a significantly higher proportion of osteocytes/

chondrocyte-positive cells compared with the differentiated NS, indicating that FC endogenously undergo differentiation toward a more mesenchymal lineage (Fig. 4E). On the other

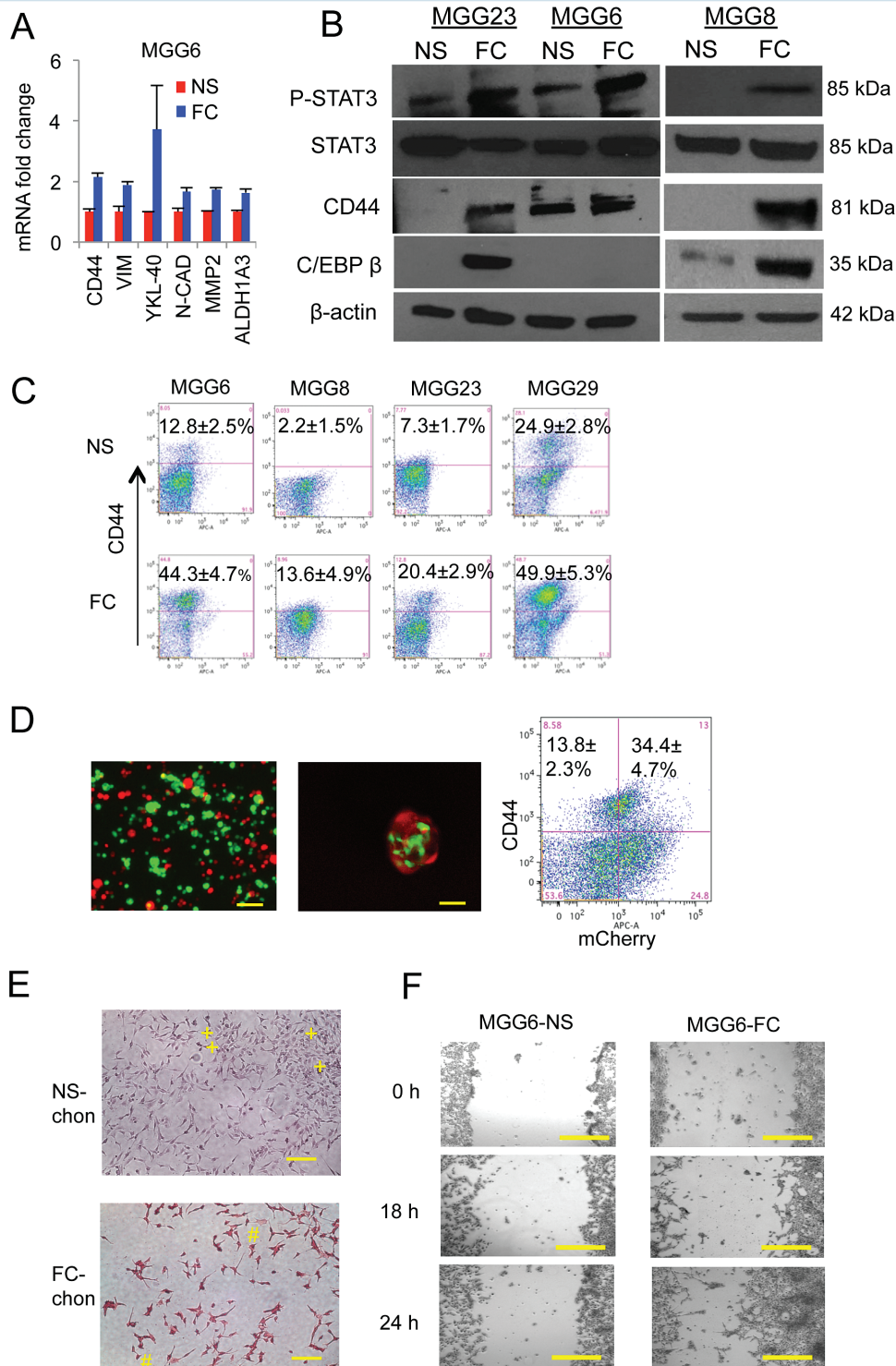


Fig. 4 Floating cells display enhanced mesenchymal properties. (A) MGG6 NS and FC mRNA were analyzed by qRT-PCR for different mesenchymal markers including CD44, vimentin, YKL-40, N-cad, and MMP2. (B) Cell lysates from different cultures were analyzed by western blotting for pSTAT3, STAT3, CD44, C/EBP β , and β -actin. (C) FACS analysis showing proportion of CD44 positive cells in FC and their corresponding NS from different GSC cultures. (D) MGG29 NS were fractionated into CD44^{high} and CD44^{low} subpopulation by FACS and predominant cells were established and labeled with GFP and mCherry, respectively. Left: fluorescence analysis of a mixture of these 2 subpopulations cultured in serum; middle: FC collected and analyzed for both GFP and mCherry; right: flow cytometry of CD44^{high} cells in both GFP and mCherry populations. (E) NS and FC were differentiated using StemPro Chondrogenesis Differentiation Kit and stained with fast green and safranin O (positive, #; negative, +). (F) NS and FC were cultured as a monolayer and their ability to invade/migrate was evaluated using scratch healing assay. Bright field micrographs are showing for different groups. Scale bar, 50 μ m.

hand, nondifferentiated NS or FC did not show any staining (Supplementary Fig. S8). Finally, using the scratch wound healing assay, we observed that FC displayed a significantly greater migration potential compared with NS, consistent with a MES phenotype (Fig. 4F and Supplementary Fig. S9).

Floating Cells Display Therapeutic Resistance

Since MES GSCs present an increased DNA damage repair capacity,^{7,9} we assessed the response of NS and FC to different known cancer therapeutics. The response to temozolomide (TMZ), the chemotherapeutic of choice for GBM, was first tested in 3 pairs of FC and NS cultures. NS from MGG6 and MGG8 were relatively sensitive to TMZ, with a half-maximal inhibitory concentration (IC_{50}) of 33 μ M and 5 μ M, respectively, while MGG23 was more resistant, with an IC_{50} of 350 μ M. In contrast, all FC demonstrated increased resistance to TMZ (relative to their parental NS), with IC_{50} of 127, 65, and >500 μ M in MGG6, MGG8, and MGG23, respectively (Fig. 5A). We further assessed the response of these cells to different doses of radiation therapy (3, 6, and 8 Gy). NS from MGG6 showed relatively higher radiosensitivity, while MGG23 had a moderate response and BT01 was relatively radioresistant. All 3 corresponding FC cultures showed a significantly higher resistance to radiation compared with parental NS (Fig. 5B). Radiation is known to block the cells in the G2/M phase. Indeed, a 6 Gy dose induced significant G2/M cell cycle arrest in all NS compared with nonradiated cells. The percentage of cells in G2/M phase were 66.3%, 45.9%, and 27.3% in radiated MGG6, MGG8, and MGG29 NS, respectively. However, the percentage of G2/M phase cells was significantly decreased in corresponding FC, with only 34.7%, 26.5%, and 19.6% in MGG6, MGG8, and MGG29, respectively (Fig. 5C, Supplementary Fig. S10). Finally, we screened the "Target Selective Inhibitor Library" on MGG23 FC and NS and assessed cell viability. Thirty-seven compounds showed a decrease in cell viability (>25%). Among them, 29 compounds (78%) showed increased resistance in FC compared with NS (Fig. 5D). We selected 6 of these hits for subsequent validation and confirmed increased therapeutic resistance in MGG8 FC compared with NS (Fig. 5E). We further assessed the effect of 3 compounds (topotecan, NVP-BEP800, and Stattic) on sphere formation using ELDA and observed that stem cell frequency in FC was significantly higher compared with NS posttreatment (Fig. 5F). These results demonstrate the increased self-renewal and treatment resistance of the FC population compared with their parental NS.

NF κ B Regulates Floating Cell Spheres Formation

Intrinsic activation of various transcription factors has been shown to promote a MES switch in cancer cells, including gliomas.^{7,13,14} Particularly, the transcription factor NF κ B, a master regulator of the cellular stress response,²⁶ promotes MES differentiation in GBM, in response to radiation.⁷ Using an NF κ B bioluminescent reporter system based on the secreted *Gaussia luciferase* (Gluc),²¹ we showed that FC had a significantly higher level of NF κ B activation compared with corresponding NS in 3 different GBM cultures (MGG6, MGG8, MGG23; Fig. 6A). These results were confirmed by

western blotting and qRT-PCR showing increased phosphorylation of p65 (ser536) and markedly higher mRNA expression of 5 NF κ B target genes (TNFAIP3 [tumor necrosis factor alpha induced protein 3], CXCL2 [C-X-C motif chemokine ligand 2], ICAM1 [intercellular adhesion molecule 1, aka CD54], IL1 β [interleukin 1beta], and NQO1 [NAD(P)H quinone dehydrogenase 1]) in FC compared with parental NS (Fig. 6B–C). To determine whether NF κ B activation is required for the generation of FC, we stably expressed GFP, along with a mutant super-repressor form of inhibitor of kappa B ($I\kappa$ B) α (GFP-mutant $I\kappa$ B α)²⁶ in NS. This mutant $I\kappa$ B α is resistant to phosphorylation and degradation, thereby inhibiting NF κ B activity in the transduced GFP(+) cells.²⁷ Proneural GSC cultures 84 and 157 were engineered to achieve approximately 30% transduction efficiency, based on GFP expression (assessed by flow cytometry), thereby generating a mixed population of GSCs expressing both wild type $I\kappa$ B α /GFP(–) and mut $I\kappa$ B α /GFP(+). These cells were subsequently attached in serum-containing medium and allowed to form FC. Remarkably, none of the FC generated showed any GFP expression (and therefore $I\kappa$ B α), suggesting that NF κ B activation is needed to generate FC (Supplementary Fig. S11).

Discussion

Substantial evidence suggests that a subset of solid tumors contain cancer stem cells which play an important role in tumor initiation, progression, metastasis, and therapeutic resistance.^{1,2} GBM stem cells in particular may possess several unique characteristics that make them resistant to conventional chemo- and radiotherapy, such as high expression of drug transporters, relative cell-cycle quiescence, high function of DNA repair machinery, and resistance to apoptosis.^{5,28} GSCs reside in a tumor niche where both the stemness status and angiogenesis are conditioned by the microenvironment, such as hypoxia, due to limited oxygen availability, and low pH caused by accumulation of acidosis products of the glycolytic metabolism. When patient-derived GSCs are cultured in serum-containing medium to induce differentiated and nontumorigenic cells, we show that a subpopulation of these tumor cells escapes adhesion/differentiation and maintains the ability to self-renew by forming secondary spheres with enhanced GSC MES properties. These results endorse intratumor molecular subtype heterogeneity in GBM, recently described using single cell RNA sequencing.¹⁰ Whether these cells are preexistent and selected from the initial "undifferentiated" NS population and subsequently enriched in FC or are dedifferentiated from mature GBM cells is debatable. The cell surface marker CD44 is highly expressed in MES GBM and could be used as a surrogate marker for this subtype.⁷ We show that both CD44^{high} and CD44^{low} GSCs can generate FC harboring high levels of CD44 with enhanced MES phenotype (irrespective of original subtype), suggesting the presence of a genetic switch as one mechanism leading to an enriched tumorigenic stem cell population in FC. Further, gliomas and GSCs tend to shift toward a more MES phenotype upon intrinsic activation of various transcription factors such as STAT3, C/EBP β , and NF κ B,^{7,9,13} all of which were increased/activated predominantly in FC. These data suggest that the

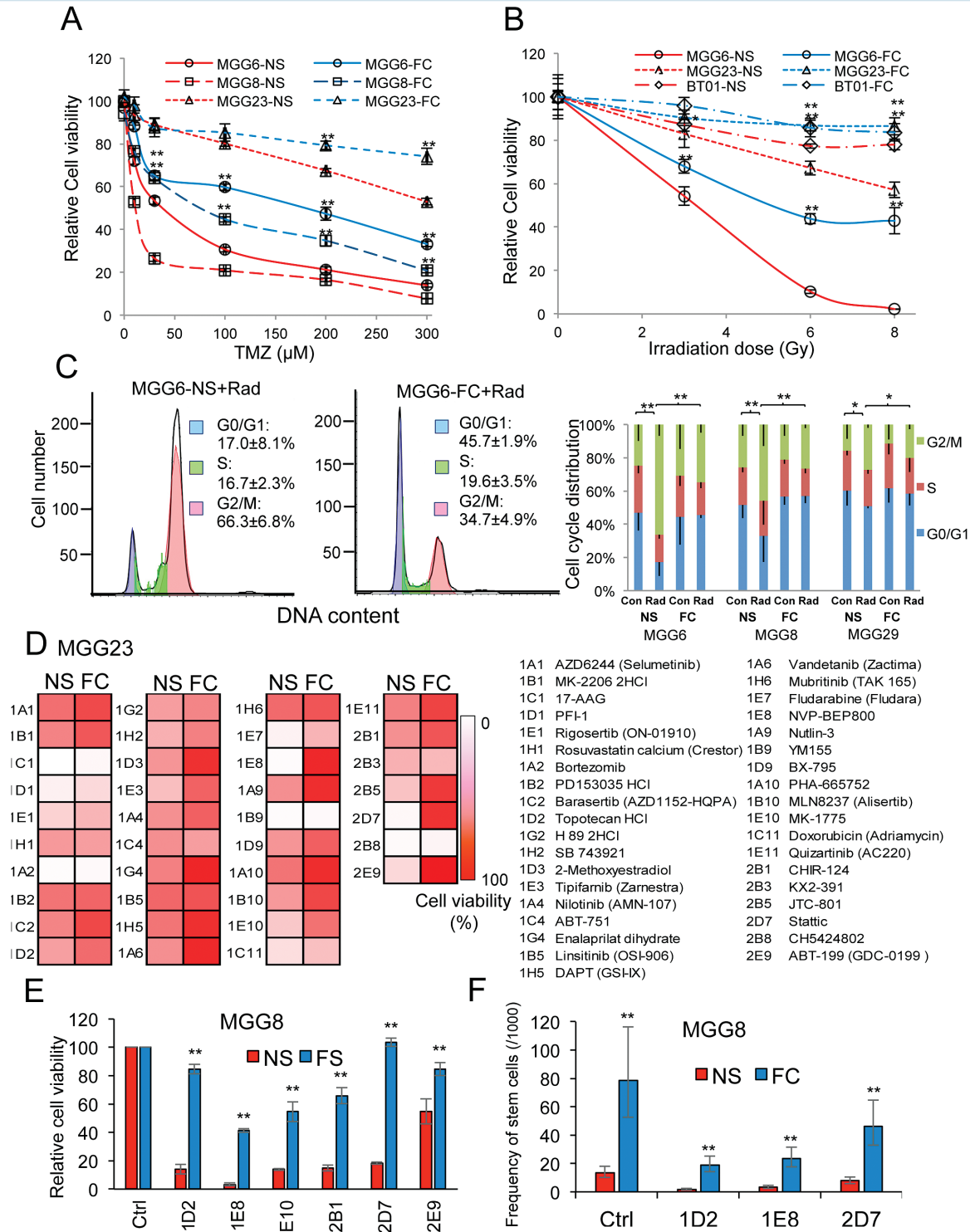


Fig. 5 Floating cells display therapeutic resistance. (A–B) NS and FC from 3 different GSC cultures were treated with increasing doses of temozolomide for 3 days (A) or radiation for 5 days (B) and analyzed for cell viability ($*P < .01$, $**P < .01$ FC vs NS). (C) Effect of 6 Gy ionizing radiation on cell cycle. Left histograms, showing a representative DNA content with propidium iodide staining in MGG6 NS and FC. Right column figure, cell cycle distribution in NS and FC from MGG6, MGG8, and MGG23 GSCs ($**P < .05$; G2/M percentage control vs radiation or NS vs FC). (D) MGG23 NS and FC were screened using the “Target Selective Inhibitor Library.” Cell viability at 72 h posttreatment is shown as gradations of red to white; white, no cell alive; red, same proportion of live cells as in vehicle control (0.1% dimethyl sulfoxide). (E) Six selected hits from the screen were validated on MGG8 NS and FC and cell viability was assessed 72 h posttreatment; $**P < .01$ FC vs NS. (F) Influence of selected drug hits on stem cell frequency (with 95% CIs) in NS and FC after one week treatment from MGG8 GSCs was evaluated using the extreme limiting dilution analysis (ELDA); $**P < .01$ FC vs NS by chi-square test.

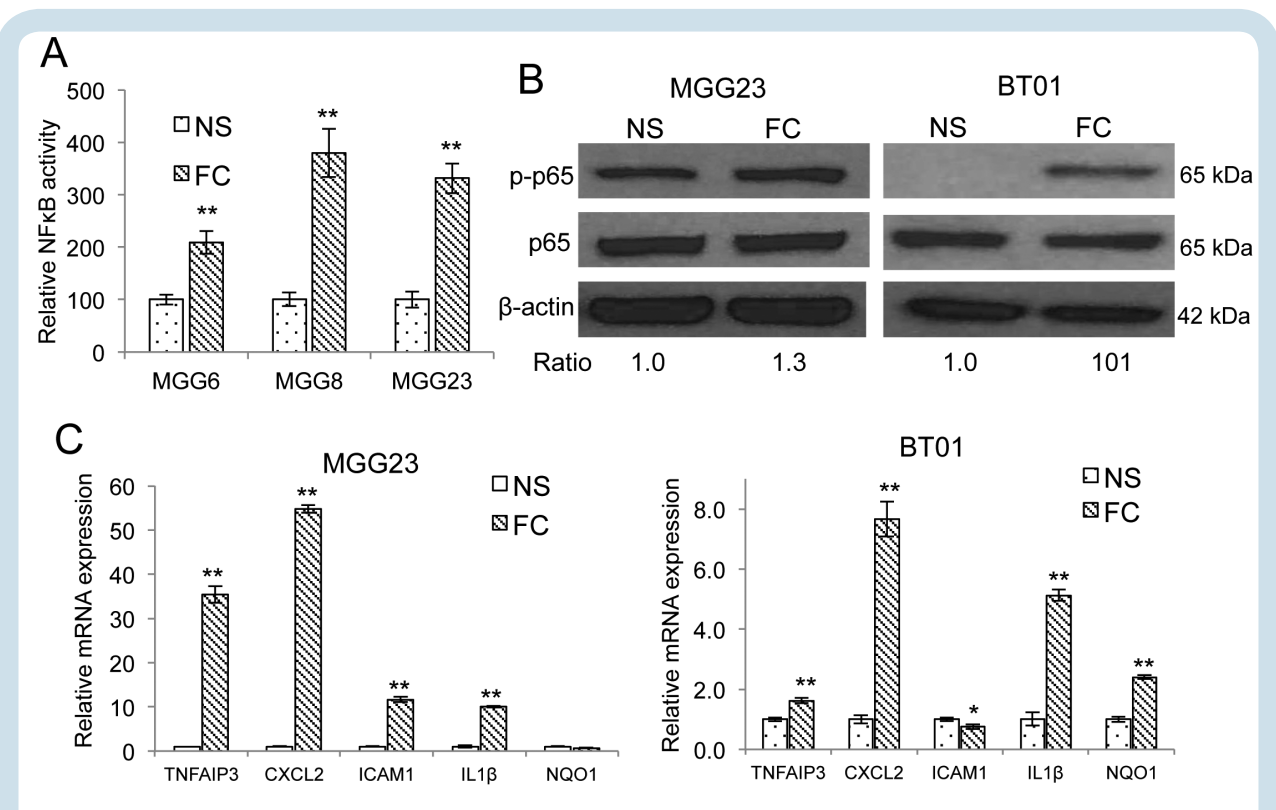


Fig. 6 NFκB activation in floating cells. (A) NS stably expressing NFκB-Gluc and SV40-Vluc were differentiated in serum and FC were collected from them. The normalized Gluc/Vluc level, a marker for NFκB activity, was analyzed in an aliquot of conditioned medium from NS and FC; ** $P < .01$ FC vs NS (mean \pm SD, $n = 8$). (B) Cell lysates from NS and FC of MGG23 and BT01 were analyzed by western blotting for phosphorylated form and total p65 (ser536) as well as β -actin ratio of p-p65 over p65 is presented. (C) NS and FC mRNA from MGG23 and BT01 were analyzed by qRT-PCR for different NFκB target genes. Fold change relative to expression in NS are presented; ** $P < .01$ FC vs NS (mean \pm SD, $n = 8$).

cell culture environment, including acidic and hypoxic conditions, results in intrinsic activation of transcription factors that promote a pro-MES switch. Previous studies have suggested that derivation of spheres from cancer cell lines or primary culture cells and extrinsic conditions such as therapeutic and/or physiological stress often lead to a phenotypic switch. This is reminiscent of an epithelial-to-mesenchymal transition (EMT) observed in a variety of tumor types and generally leads to increased invasiveness and acquired resistance to various environmental insults.²⁹

GSCs isolated from MES GBM tumors tend to lose their MES properties and present a PN signature once grown in NS-forming culture conditions, even at early passages *in vitro*.⁷ This loss of MES identity has been attributed to the change of tumor microenvironment that is likely to promote and maintain MES properties. Acidic extracellular pH and low oxygen tension are major pathophysiological features in solid tumor tissues, primarily due to lactate secretion from anaerobic glycolysis, and have been suggested to promote local invasion.³⁰ Neutralizing acidic pH with sodium bicarbonate has been shown to increase the therapeutic response to chemotherapy and to inhibit metastasis.³¹ In the case of malignant gliomas, acidic stress (pH 6.6) is partly responsible for promoting a GSC phenotype and increasing vascular endothelial growth factor expression, which typically correlates with tumor progression.²⁵ Electrode measurements of

pH in human brain tumors demonstrated a pH as low as 5.9 with a mean around 6.8, with the normal brain tissue having a pH of ~ 7.1 .^{25,32} In contrast, cell culture media, including NBM, which are widely applied to grow GSCs, have a slightly alkaline pH at baseline and are designed to maintain neutral pH during cellular growth. Our results suggest that low pH through secretion of lactic acid in the conditioned medium is a major contributor in maintaining GBM intratumor molecular subtype heterogeneity and MES switch in culture and that low oxygen potentially facilitates these phenomena. Considering our findings and other studies linking hypoxia to GSCs, cell culture under reduced oxygen tension and pH might be more appropriate to enable *in vitro* maintenance of the physiologically relevant inherent cellular heterogeneity found in GBM.³³

Recently, invasive circulating tumor cells with MES properties have been identified for the first time in peripheral blood samples of glioma patients.³⁴ This finding reinforces the idea that an EMT-like process does occur in GBM patients as well. It remains to be determined whether the similarities between the FC from primary GBM cultures and circulating tumor cells from GBM patients extend beyond the phenotypic resemblance (loss of adhesion) and gain of MES properties. More studies will also help determine whether MES transition in FC is complete or reversible following long-term culture in standard stem cell culture conditions. GSCs

with MES properties present a more aggressive phenotype both in culture and in vivo, along with a pronounced radioresistance.^{7,9} Further, plasticity between PN to a MES phenotype is observed upon GBM recurrence, or in response to radiation therapy.^{7,9,12} Thus, in vitro modeling of MES transition could be highly beneficial in understanding the main drivers of this switch that leads to treatment resistance or tumor recurrence.^{35,36} While further characterization of the FC population is needed in order to assess their clinical relevance, the aggressive phenotype and enhanced therapeutic resistance of these cells make them a valuable model to maintain/study intratumor heterogeneity and GSC plasticity and to test novel therapeutics aiming at eradicating GBM in general and GSCs in particular.

Conclusions

Patient-derived GBM stemlike cells undergo differentiation when cultured in serum-containing medium; however, a small subpopulation of these cells escapes this adhesion/differentiation and grow as floating cells. These cells revealed enhanced GSC properties with MES genotype/phenotype along with increased migration/invasion, resistance to therapy, and tumor formation in vivo. Our findings support GBM inherent intratumor molecular subtype heterogeneity as well as GSC plasticity, which could have significant clinical implications.

Supplementary Material

Supplementary material is available at *Neuro-Oncology* online.

Funding

This work was supported by grants from the National Institutes of Health, the National Institute of Neurological Disorders R01NS064983, 1R01NS095647 and P30NS04776 (B.A.T.) and the National Cancer Institute R01CA166077 (B.A.T.), 2P01CA069246 (B.A.T. and E.N.C.) and K22CA197053 (C.E.B.).

Acknowledgments

The authors acknowledge the MGH Neuroscience Image Analysis Core (for confocal microscopy), and the MGH Vector Core (for producing the viral vector) supported by NIH/NINDS P30NS04776 (B.A.T.) as well as 1S10RR025504 Shared Instrumentation grant for the IVIS imaging system.

Conflict of interest statement. The authors declare no competing financial interests.

References

- Omuro A, DeAngelis LM. Glioblastoma and other malignant gliomas: a clinical review. *JAMA*. 2013;310(17):1842–1850.
- Carlsson SK, Brothers SP, Wahlestedt C. Emerging treatment strategies for glioblastoma multiforme. *EMBO Mol Med*. 2014;6(11):1359–1370.
- Nathanson DA, Gini B, Mottahedeh J, et al. Targeted therapy resistance mediated by dynamic regulation of extrachromosomal mutant EGFR DNA. *Science*. 2014;343(6166):72–76.
- Singh SK, Clarke ID, Terasaki M, et al. Identification of a cancer stem cell in human brain tumors. *Cancer Res*. 2003;63(18):5821–5828.
- Bonavia R, Inda MM, Cavenee WK, et al. Heterogeneity maintenance in glioblastoma: a social network. *Cancer Res*. 2011;71(12):4055–4060.
- Wang R, Chadalavada K, Wilshire J, et al. Glioblastoma stem-like cells give rise to tumour endothelium. *Nature*. 2010;468(7325):829–833.
- Bhat KP, Balasubramanian V, Vaillant B, et al. Mesenchymal differentiation mediated by NF- κ B promotes radiation resistance in glioblastoma. *Cancer Cell*. 2013;24(3):331–346.
- Gill BJ, Pisapia DJ, Malone HR, et al. MRI-localized biopsies reveal subtype-specific differences in molecular and cellular composition at the margins of glioblastoma. *Proc Natl Acad Sci U S A*. 2014;111(34):12550–12555.
- Mao P, Joshi K, Li J, et al. Mesenchymal glioma stem cells are maintained by activated glycolytic metabolism involving aldehyde dehydrogenase 1A3. *Proc Natl Acad Sci U S A*. 2013;110(21):8644–8649.
- Patel AP, Tirosh I, Trombetta JJ, et al. Single-cell RNA-seq highlights intratumoral heterogeneity in primary glioblastoma. *Science*. 2014;344(6190):1396–1401.
- Phillips HS, Kharbanda S, Chen R, et al. Molecular subclasses of high-grade glioma predict prognosis, delineate a pattern of disease progression, and resemble stages in neurogenesis. *Cancer Cell*. 2006;9(3):157–173.
- Mahabir R, Tanino M, Elmansuri A, et al. Sustained elevation of Snail promotes glial-mesenchymal transition after irradiation in malignant glioma. *Neuro Oncol*. 2014;16(5):671–685.
- Carro MS, Lim WK, Alvarez MJ, et al. The transcriptional network for mesenchymal transformation of brain tumours. *Nature*. 2010;463(7279):318–325.
- Mikheeva SA, Mikheev AM, Petit A, et al. TWIST1 promotes invasion through mesenchymal change in human glioblastoma. *Mol Cancer*. 2010;9:194.
- Suvà ML, Rheinbay E, Gillespie SM, et al. Reconstructing and reprogramming the tumor-propagating potential of glioblastoma stem-like cells. *Cell*. 2014;157(3):580–594.
- Rheinbay E, Suvà ML, Gillespie SM, et al. An aberrant transcription factor network essential for Wnt signaling and stem cell maintenance in glioblastoma. *Cell Rep*. 2013;3(5):1567–1579.
- Lee J, Kotliarova S, Kotliarov Y, et al. Tumor stem cells derived from glioblastomas cultured in bFGF and EGF more closely mirror the phenotype and genotype of primary tumors than do serum-cultured cell lines. *Cancer Cell*. 2006;9(5):391–403.
- Wakimoto H, Kesari S, Farrell CJ, et al. Human glioblastoma-derived cancer stem cells: establishment of invasive glioma models and treatment with oncolytic herpes simplex virus vectors. *Cancer Res*. 2009;69(8):3472–3481.
- Wakimoto H, Mohapatra G, Kanai R, et al. Maintenance of primary tumor phenotype and genotype in glioblastoma stem cells. *Neuro Oncol*. 2012;14(2):132–144.
- Wurdinger T, Badr C, Pike L, et al. A secreted luciferase for ex vivo monitoring of in vivo processes. *Nat Methods*. 2008;5(2):171–173.

21. Badr CE, Niers JM, Tjon-Kon-Fat LA, et al. Real-time monitoring of nuclear factor kappaB activity in cultured cells and in animal models. *Mol Imaging*. 2009;8(5):278–290.
22. Maguire CA, Bovenberg MS, Crommentuijn MH, et al. Triple bioluminescence imaging for in vivo monitoring of cellular processes. *Mol Ther Nucleic Acids*. 2013;2:e99.
23. Tannous BA. Gaussia luciferase reporter assay for monitoring biological processes in culture and in vivo. *Nat Protoc*. 2009;4(4):582–591.
24. Hu Y, Smyth GK. ELDA: extreme limiting dilution analysis for comparing depleted and enriched populations in stem cell and other assays. *J Immunol Methods*. 2009;347(1-2):70–78.
25. Hjelmeland AB, Wu Q, Heddlestone JM, et al. Acidic stress promotes a glioma stem cell phenotype. *Cell Death Differ*. 2011;18(5): 829–840.
26. Boehm JS, Zhao JJ, Yao J, et al. Integrative genomic approaches identify IKBKE as a breast cancer oncogene. *Cell*. 2007;129(6): 1065–1079.
27. Brown K, Gerstberger S, Carlson L, et al. Control of I kappa B-alpha proteolysis by site-specific, signal-induced phosphorylation. *Science*. 1995;267(5203):1485–1488.
28. Diehn M, Clarke MF. Cancer stem cells and radiotherapy: new insights into tumor radioresistance. *J Natl Cancer Inst*. 2006;98(24):1755–1757.
29. Kalluri R, Weinberg RA. The basics of epithelial-mesenchymal transition. *J Clin Invest*. 2009;119(6):1420–1428.
30. Tannock IF, Rotin D. Acid pH in tumors and its potential for therapeutic exploitation. *Cancer Res*. 1989;49(16):4373–4384.
31. Estrella V, Chen T, Lloyd M, et al. Acidity generated by the tumor microenvironment drives local invasion. *Cancer Res*. 2013;73(5):1524–1535.
32. Kato Y, Ozawa S, Miyamoto C, et al. Acidic extracellular microenvironment and cancer. *Cancer Cell Int*. 2013;13(1):89.
33. Ricci-Vitiani L, Pallini R, Biffoni M, et al. Tumour vascularization via endothelial differentiation of glioblastoma stem-like cells. *Nature*. 2010;468(7325):824–828.
34. Sullivan JP, Nahed BV, Madden MW, et al. Brain tumor cells in circulation are enriched for mesenchymal gene expression. *Cancer Discov*. 2014;4(11):1299–1309.
35. Appaix F, Nissou MF, van der Sanden B, et al. Brain mesenchymal stem cells: The other stem cells of the brain? *World J Stem Cells*. 2014;6(2):134–143.
36. Kemper K, de Goeje PL, Peeper DS, et al. Phenotype switching: tumor cell plasticity as a resistance mechanism and target for therapy. *Cancer Res*. 2014;74(21):5937–5941.